

A Novel Meteorological Method to Classify Wintertime Cold-Air Pool Events

Sean Colgan¹, Xia Sun^{2,3} and Heather Holmes^{4*}

¹ *Atmospheric Sciences Program, Department of Physics, University of Nevada, Reno, Reno, NV*

² *Cooperative Institute for Research in Environmental Sciences, University of Colorado Boulder*

³ *NOAA/Global Systems Laboratory, Boulder, Colorado*

⁴ *Department of Chemical Engineering, University of Utah, Salt Lake City, UT*

**Corresponding Author: 50 S. Central Campus Dr. MEB 3290, Salt Lake City, UT 84112-9203,*

+1-801-581-3248, h.holmes@utah.edu

Highlights:

- PM_{2.5} concentration increases with CAPs but magnitude varies across locations
- Synoptic meteorology determines CAP onset and local meteorology determines duration
- New method was developed to classify CAPs relying only on local meteorology data
- Radiosondes released above the valley floor underestimate CAP strength more than 30%
- Surface station meteorological data can complement radiosonde data to quantify CAPs

Abstract:

Cold air pools (CAPs) are common in mountain valleys throughout the world (e.g., western North America, Himalayas, Alps, etc.) during winter months. Weak surface winds, cold temperatures, high humidity, and snow cover presence are common characteristics of CAPs, and in populated areas there is an increase in air pollution concentrations. Previous methods for identifying CAP events and determining their strength often rely on a combination of, radiosonde data, air pollution concentrations, and/or surface meteorological datasets. Ambient air pollution concentrations vary by location based on the local emissions sources and continually change due to regulations, therefore they are unreliable for consistent CAP quantification. Here, the bulk atmospheric stability is calculated as the valley heat deficit (VHD) using radiosonde data for 12 locations in the western U.S. over 16 winters. A new CAP classification method is developed and compared to three existing CAP classification methods. Results indicate that the new method agrees well with existing approaches but provides a more robust CAP classification because it is solely based on meteorology and not air quality. For all locations, 00Z (afternoon/early evening)

32 radiosondes account for roughly 20-40% of all CAP occurrences (12Z and 00Z), independent of
33 the method used. Meaning that the stable boundary layer persists throughout the daytime in these
34 cases often leading to persistent CAP events (PCAP). While PCAP length varies across
35 locations, they are a similar order of magnitude because synoptic conditions that span the entire
36 western U.S. govern CAP formation and PCAP length. Additionally, several locations (e.g.,
37 Reno, Elko, Spokane, Riverton, and Grand Junction) release radiosondes above the valley floor,
38 often underestimating the bulk atmospheric stability by more than 30%. A method to incorporate
39 surface station data in the bulk atmospheric stability calculation is given to reduce this
40 underestimation.

41

42 **Keywords:**

43 Stable stratification; Mountain meteorology; Climatology; Radiosonde; Air quality; PM_{2.5}

44

45 **1. Introduction**

46 Cold air pools (CAPs) often occur in areas with valleys and basins in the western U.S.
47 during winter months due to shallow, stably stratified atmospheric boundary layers (ABLs)
48 (Whiteman et al., 2014). CAPs are defined as the topographic depression filled with cold air with
49 warm air overlying above. CAPs can be classified as diurnal, lasting for less than one day, and
50 persistent, lasting for days or even weeks (Whiteman et al., 2001). Diurnal CAPs are formed due
51 to the effective surface radiative cooling at night and decay after sunrise with increased incoming
52 solar radiation. Persistent CAPs (PCAPs) occur when the surface heating is not strong enough to
53 mix out the stratified atmospheric layers in the afternoon. The presence of a PCAP can cause
54 serious air pollutant accumulations in mountainous valleys. During PCAPs, PM_{2.5} (particulate
55 matter with a diameter of less than 2.5 μm) can steadily increase by 10 μg m⁻³ per day, reaching
56 or exceeding the 24-hr PM_{2.5} National Ambient Air Quality Standard (NAAQS) of 35 μg m⁻³
57 (Holmes et al., 2015; Silcox et al., 2012; Whiteman et al., 2014). The health impacts of air
58 pollution exposure during CAPs have the potential to linger for a month or longer, affecting the
59 cardiovascular and respiratory systems (Zanobetti et al., 2003).

60 The evolution of a CAP can be summarized as four stages: formation, disturbance,
61 persistence, and break-up (Lareau and Horel 2015a). The formation of a CAP occurs under
62 stagnant synoptic patterns (e.g., an incoming ridge from the west), which produce a pool of cold

63 air at the surface with warm air aloft. The high-pressure/ridge leads to subsidence (sinking
64 motions) that traps the cooler air near the surface and warmer air aloft. The disturbance,
65 persistence and break-up stages are impacted by local factors, like lake breezes (e.g., in the Salt
66 Lake Valley), shortwaves (cold air advection aloft), and turbulence in the lower/middle
67 atmosphere (Lareau and Horel 2015b). For example, sufficiently large surface sensible heat
68 fluxes in the afternoon can destroy the CAP by transporting heat from the ground to the ABL,
69 leading to a breakdown of the stable stratification, namely the dry convection mechanism. In the
70 presence of strong winds aloft, it is possible for the CAP to be removed by turbulent erosion
71 starting from the mountain top and then penetrating downwards into the valley air over time.
72 CAP displacement represents the re-arrangement process of CAP mass caused by dynamic and
73 static processes, such as a mountain wave. It is sometimes the interactions of these mechanisms
74 that lead to the final removal of a CAP. Intermittent weak perturbations between the stages
75 occurs when these mechanisms only weaken but not fully destroy the CAP. Alternatively, snow
76 cover strengthens a CAP with increased surface albedo and reduced surface net radiation.

77 Low-level clouds impact the thermodynamic structure of the ABL and the surface energy
78 balance, and both have implications on the CAP strength and duration. Holmes et al., (2015)
79 used the terms ‘dry CAP’ and ‘cloudy CAP’ to discuss the boundary layer cloud impacts. They
80 found that the cloudy CAPs enhanced turbulence in the boundary layer due to the cloud top-
81 down mixing impact. Boundary layer clouds modulate the surface radiation budget by reducing
82 the incoming solar radiation and emitting longwave radiation. Cloud top entrainment can induce
83 cloud internal turbulence and affect ABL structure (Deardorff 1970). Radiative cooling at the
84 cloud top also contributes to turbulence production in the boundary layer (Shin and Ha 2009).
85 Holmes et al., (2015) observed higher surface sensible heat fluxes under cloudy CAP with a
86 lower valley heat deficit compared with dry CAP, suggesting a decrease in atmosphere stability.
87 Additionally, the PM_{2.5} concentrations during a cloudy CAP were slightly lower than the dry
88 CAP due to the enhanced vertical mixing. Understanding the key factors impacting CAPs and
89 their interactions during CAP evolution are expected to provide information for potential
90 numerical model developments and ultimately forecasting improvements.

91 There have been several field campaigns focusing on CAPs. A meteorological field
92 experiment was conducted in a small basin in the United Kingdom (UK) from October 2001 to
93 June 2002 (Jemmet-Smith et al., 2019). Their goals were to better understand temperature and

94 wind flow patterns during CAPs in the Clun Valley, UK (a shallow valley of 100-200-meter
95 depth). The Persistent Cold Air Pool Study (PCAPS) was conducted in the northern Utah from
96 December 2010 to February 2011 (Lareau et al., 2013). There were ten persistent CAPs observed
97 during this winter field campaign with unique meteorological and surface energy balance
98 datasets for analysis. The Yakima Air Wintertime Nitrate Study (YAWNS), focusing on the
99 elevated air pollution levels during wintertime CAPs, was conducted Yakima, Washington from
100 5 to 27 January 2013 (VanReken et al., 2017). In addition, there are several individual studies
101 focusing on CAPs in other basin areas, such as California's Central Valley in U.S. (Wilson and
102 Fovell 2018), the Danube Valley in Germany (Zängl 2005), and the Po Valley in Italy (Hoggarth
103 et al., 2006). Largely, these studies have been motivated by the significance of CAPs in
104 mountainous regions during the winter months due to an abundance of unhealthy particulate
105 matter accumulating near the surface.

106 Multiple CAP classification methods have been presented in literature. Each method uses
107 different datasets and thresholds to determine the CAPs. These methods have explored using
108 observations and reanalysis data. Yu et al., (2017) used gridded reanalysis datasets to identify
109 valley cold pools (VCPs) using lapse rates to determine the presence of deep stable layers
110 (Wolyn and McKee 1989) and a 10-m wind speed threshold. There have been multiple
111 observational studies conducted in the Salt Lake Valley (SLV) over the past decade (Baasandorj
112 et al., 2017; Lareau et al., 2013; Franchin et al., 2018; Ivey et al., 2019; Silcox et al., 2012; Sun
113 and Holmes 2019; Whiteman et al., 2014), where industry and vehicle air pollution emissions
114 and topography lead to pollutant accumulation and prolonged stable boundary layers under the
115 unfavorable synoptic conditions. The elevated, wintertime air pollution concentrations in the
116 SLV have been associated with adverse cardiorespiratory health outcomes (Pope III, 1991; Pope
117 III et al., 2006).

118 In this paper, we investigate the differences between CAP classification methods from
119 Whiteman et al., (2014), Pierce et al., (2019), and Yu et al., (2017) using data during wintertime
120 (i.e., October-March) from 2002-2018 in 12 valley locations at western U.S. The goals of this
121 study are to improve the vertical meteorological data record where the radiosonde is released
122 above the valley floor, evaluate the existing methods to classify CAP events, and develop a new
123 CAP classification method that can be applied to any location. A universal method for

124 identifying CAPs is needed to determine the duration and strength of stagnation across multiple
125 valleys in a region and reduce ambiguity in CAP classification methods.
126

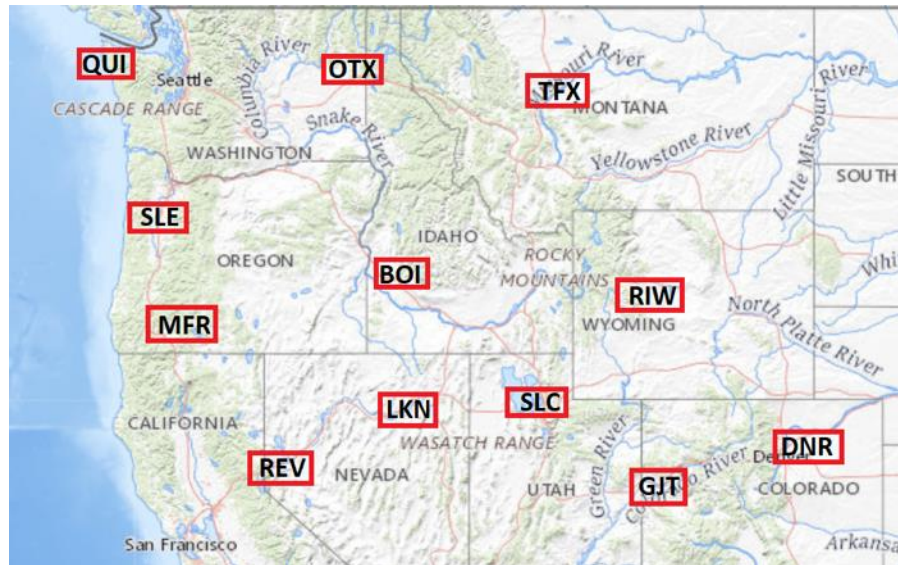


Figure 1. **Map of 12 Radiosonde Locations.** Boise, ID (BOI); Salt Lake City, UT (SLC); Reno, NV (REV); Medford, OR (MFR); Salem, OR (SLE); Denver, CO (DNR); Spokane, WA (OTX); Grand Junction (GJT); Elko, NV (LKN); Great Falls, MT (TFX); Riverton, WY (RIW); Quillayute, WA (QUI).
Map from: <https://viewer.nationalmap.gov/advanced-viewer/>

127

128 2. Data

129 Observational data from radiosondes, weather stations, and air quality monitors in 12
130 locations in the western U.S. (Figure 1) were used. This study extends previous CAP studies by
131 investigating CAPs in multiple locations using observations. Using all available radiosonde data
132 across the mountainous western U.S. provides results for locations where CAP events have not
133 been previously studied (e.g., Elko, Salem, and Riverton). This analysis provides an
134 observational quantification of CAP events that can be compared with CAP classifications from
135 gridded reanalysis products in future studies.

136

137 2.1 Radiosonde

138 Radiosonde data from October 1, 2002 to March 31, 2018 were obtained online from the
139 University of Wyoming (<http://weather.uwyo.edu/upperair/sounding.html>). The stations used to
140 develop and evaluate new metrics for CAP classification are shown in Figure 1 and Table 1. The
141 elevation difference between the valley floor and radiosonde launch site (Table 1) results in

142 missing data for the purpose of CAP identification (i.e., when the radiosonde is released above
 143 the valley floor, there is a section of the atmosphere not accounted for in the radiosonde data
 144 record). The radiosonde data, including vertical profiles of temperature, dewpoint temperature,
 145 pressure and wind, were used to classify CAP events based on the methods described below in
 146 Section 3. Mean ridge heights for each valley were determined using a topographic available
 147 online from the United States Geological Survey (<https://viewer.nationalmap.gov/advanced-viewer/>). Mean ridge heights are important for identifying CAPs because the depth of the stable
 148 atmospheric boundary layer is below the ridge heights due to the blocking effect caused by the
 149 upwind mountains.
 150

151 Table 1. Elevations (m MSL) of valley floor, mean ridge height, and radiosonde launch site for 12 locations in the
 152 western United States and the amount of missing data in the vertical profile obtained from the radiosonde (i.e.,
 153 elevation difference between radiosonde site and valley floor).
 154

Location	Valley Floor (m MSL)	Mean Ridge Height (m MSL)	Radiosonde Site (m MSL)	Missing Data (m)
BOI	830	1829	874	44
SLC	1289	2438	1289	0
REV	1342	2134	1516	174
MFR	400	1219	405	5
SLE	47	914	61	14
DNR	1611	2743	1611	0
OTX	595	1829	728	133
GJT	1397	2743	1475	78
LKN	1540	2438	1608	68
TFX	1015	2134	1134	119
RIW	1509	2743	1703	194
QUI	59	914	62	3

155

156 2.2 Surface Meteorology

157 Surface meteorological data were collected at the three locations where radiosondes are
 158 released above the valley floor: Reno (KRNO), Elko (KEKO), and Spokane (KSFF). These
 159 locations use Automated Surface Observing Stations (ASOS) and the ASOS data were obtained
 160 through MESOWEST (<https://mesowest.utah.edu/>) (Horel et al., 2002), and followed by quality
 161 control checks. For example, station pressure was recorded as mean sea level pressure prior to
 162 2014 for all locations and the altimeter was being recorded as station pressure during that time

163 frame. The ASOS data on the valley floor were appended to the radiosonde data as the lowest
164 elevation at 00Z and 12Z.

165

166 *2.3 Air Pollution*

167 $PM_{2.5}$ data were used to investigate the relationship between the bulk atmospheric
168 stability and air pollution concentrations during CAP events. $PM_{2.5}$ concentration data were
169 collected from the U.S. Environmental Protection Agency (EPA) Air Quality System (AQS)
170 network for cities with EPA monitors (<https://www.epa.gov/outdoor-air-quality-data>). Stable
171 atmospheric boundary layer events lead to increased $PM_{2.5}$ concentrations near the surface
172 because of the inability for air parcels to rise and the lower boundary layer heights which leads to
173 less turbulent mixing and a decreased mixing volume, respectively (Holmes et al., 2015; Silcox
174 et al., 2012; Whiteman et al., 2014.). Investigating the relationship between atmospheric stability
175 and pollutant concentrations across the western U.S. is important to determine how the local
176 topography and air population emissions influence the $PM_{2.5}$ concentrations during CAP events.
177 Three cities (Elko, NV; Quillayute, WA; and Riverton, WY) do not have EPA monitors for the
178 time period of this study, thus analyses of bulk atmospheric stability and $PM_{2.5}$ concentrations
179 were not conducted for these locations.

180

181 3. Methods

182 Previous studies typically focused on a single valley, like the Columbia Basin, Snake
183 River Valley, and the Salt Lake Valley (SLV), while few have focused on CAP events that occur
184 across a large region encompassing many valleys. For example, Whiteman et al., (2014)
185 developed a threshold using bulk stability and air pollution that is specific to the SLV. While Yu
186 et al., (2017) used reanalysis data to determine the frequency of CAP events across the western
187 U.S. Every valley in the western U.S. experiences similar synoptic meteorology that leads to the
188 formation of CAPs. However, each valley is unique with respect to local topography (e.g.,
189 blocking pattern induced by topography, prevailing winds at the surface, etc.) and the amount of
190 air pollution emissions. Here, we evaluate three CAP classification methods (Section 3.1, 3.2,
191 and 3.3) and propose a new method (Section 3.4) that can be applicable to all locations. The new
192 method relies on physical (i.e., meteorological) variables that are related to the CAP behavior
193 and is independent of air pollution concentrations.

194 *3.1 Valley Heat Deficit with PM_{2.5} Threshold (Whiteman et al., 2014)*

195 The valley heat deficit (VHD, H_h) is a measure of the bulk atmospheric stability for a
196 valley (Whiteman et al., 1999):

197

$$198 \quad H_h = c_p \int_{sfc}^h \rho(z) [\theta_h - \theta(z)] dz \quad (1)$$

199

200 Where c_p is the specific heat of air ($1005 \text{ J kg}^{-1}\text{K}^{-1}$), h is the integration height, ρ is the density of
201 air, θ is potential temperature and z is the height above ground level. A VHD threshold for Salt
202 Lake City was determined based on a 40-year climatology of VHD and $\text{PM}_{2.5}$ concentrations
203 (Whiteman et al., 2014). The VHD threshold can be used to identify the onset of a CAP episode.
204 A persistent CAP occurs when the VHD is above the threshold for at least 3 consecutive
205 soundings (i.e., more than one day). However, the threshold in Whiteman et al., (2014) is
206 specific to SLV. Each valley location would require its own climatological assessment of the
207 VHD and $\text{PM}_{2.5}$ relationship to establish the VHD threshold.

208 Whiteman et al., (2014) used a $\text{PM}_{2.5}$ concentration of $17.5 \mu\text{g m}^{-3}$ (half of the NAAQS
209 for $\text{PM}_{2.5}$) to determine the VHD threshold that identifies CAP events in SLV (hereafter referred
210 to as VHD_17.5). Here, a similar approach is taken to determine if this VHD and air quality
211 method can be applied to other valleys in the Intermountain West. The limitation of this
212 NAAQS-based $\text{PM}_{2.5}$ threshold is that the different magnitudes of ambient air pollution
213 concentration in each city associated with different amounts of emissions will lead to
214 inconsistent VHD thresholds. Additionally, with the exception of 2016-2020, $\text{PM}_{2.5}$
215 concentrations have been declining in the U.S. due to the regulations on industrial and vehicle
216 emissions (Clay and Muller 2019). Therefore, another VHD threshold for CAP events based on
217 $\text{PM}_{2.5}$ statistics, rather than the absolute $\text{PM}_{2.5}$ values, is necessary.

218

219 *3.2 Valley Heat Deficit with 75th Percentile PM_{2.5} (Pierce et al., 2019)*

220 To establish another VHD threshold value, the 75th percentile 24-hour $\text{PM}_{2.5}$
221 concentration is used in locations where air quality data was available. $\text{PM}_{2.5}$ above the 75th
222 percentile represent polluted values for that specific location and can attributed to CAP event
223 during the winter months. This method was adapted from Pierce et al., (2019), to identify
224 polluted days their study highlighted that the 75th percentile $\text{PM}_{2.5}$ concentration separates typical

225 air pollution days from days that experience elevated air pollution concentrations in Reno, NV
226 (i.e., increased air pollution due to wildfires or CAPs). The 75th percentile PM_{2.5} concentrations
227 are used in this study as a threshold to calculate a unique VHD threshold for each location
228 (hereafter referred to as VHD_75). The mean VHD is obtained from days when the 24-hr PM_{2.5}
229 concentration exceeds the 75th percentile PM_{2.5}, then this mean VHD is used as a threshold for
230 identifying CAP events. While this approach no longer uses a static PM_{2.5} concentration
231 threshold to establish a VHD threshold for CAPs, it still relies on air pollution concentrations and
232 not meteorological data.

233

234 *3.3 Valley Cold Pools (Yu et al., 2017) based on Deep Stable Layers (Wolyn and McKee 1989)*

235 Deep stable layers (DSLs) are abnormally deep stable nocturnal boundary layers that are
236 of at least moderate stability with effective stagnation in the lower atmosphere (Wolyn and
237 McKee 1989). DSLs are defined with a temperature lapse rate less than 2.5 K km⁻¹ for at least
238 65% of the lowest 1500-m AGL layer. Requiring greater than 975 m of the lower atmosphere to
239 reach this criterion often ignores stable layers with effective stagnation in the lower atmosphere
240 that do not meet the definition (Wolyn and McKee 1989). Yu et al., (2017) used the North
241 America Regional Reanalysis (NARR) dataset to identify valley cold pool (VCP) events using
242 the criteria of DSLs in Wolyn and McKee (1989), combined with a 10-m wind speed threshold
243 of less than 3 m s⁻¹ for VCP classification.

244 This method is used in this study (hereafter referred to as VCP) and these criteria are
245 applied to morning and afternoon soundings, unlike Wolyn and McKee (1989) who applied their
246 criterion to only morning soundings. Yu et al., (2017) acknowledged that they likely
247 underestimated the number of VCP in their study due to strict criteria applied to NARR, given
248 the coarse resolution (32-km horizontal and 29 vertical levels) and applying this criterion to
249 afternoon soundings. Despite that, VCP was a common weather phenomenon in the western
250 U.S., with events longer than 7 days occurring in the Columbia Basin, Snake River Basin and
251 Bonneville Basin (Yu et al., 2017).

252

253 *3.4 Novel CAP Classification Method*

254 Due to the limitations of prior approaches, there is a critical need to develop a universal
255 method that relies on the physical variables of CAP meteorology and is independent of the air

256 pollution concentrations. Ideally, the universal method can also be applied to locations without
257 radiosonde data using girded reanalysis datasets to obtain the vertical atmospheric profiles.
258 However, the focus of this paper is on developing and evaluating this new method using
259 radiosonde observations, since additional assimilation uncertainties exist in reanalysis datasets.

260 In the western U.S., the onset of a CAP episode occurs when an approaching synoptic-
261 scale ridge (i.e., surface high pressure) settles over the Intermountain West, resulting in
262 increasing surface pressure, decreasing wind speeds near the surface, and increased VHD. These
263 physical variables are attributed to stagnation in the lower atmosphere and can be used to
264 identify CAP events. We use these variables to develop a new, universal CAP classification
265 method. The new classification method still relies on the VHD from Whiteman et al., (1999), but
266 establishes the VHD thresholds based on local meteorology, instead of air quality. We use
267 surface pressure and wind speed to determine the VHD threshold value for CAP events.
268 Normalized station pressure is used to determine high pressure systems by calculating the
269 median station pressure for each location and dividing the ambient station pressure by the
270 median station pressure. Then a median VHD threshold is obtained when the normalized
271 pressure and 10-m wind speed are greater than 1.0 and less than 3 m s^{-1} , respectively. When the
272 normalized pressure is greater than 1.0, a higher surface pressure than normal is observed and
273 has potential to indicate stagnation near the surface. Since higher pressure at the surface is not
274 always indicative of stagnation, the 10-m wind speed threshold of 3 m s^{-1} isolates the stagnation
275 days from non-stagnation days. This new CAP threshold (hereafter referred to as VHD_met)
276 does not rely on the air pollution concentrations and is based purely on the meteorological
277 processes that occur in each valley.

278 While this method provides a new VHD threshold for CAP events the calculation still
279 requires location specific information that impacts the VHD magnitude (e.g., integration heights
280 in Equation 1). To extend this method and provide a VHD value that is comparable across all
281 locations, the VHD is normalized by a standard VHD value for each sounding. To obtain a
282 standard VHD, the moist adiabatic lapse rate (MALR) is used (e.g., Whiteman et al., 2014). The
283 MALR VHD is calculated for each radiosonde dataset using a standard tropospheric lapse rate of
284 $0.0065^\circ\text{C m}^{-1}$ (NOAA 1976). Then the VHD is divided by the MALR VHD to provide a non-
285 dimensional value of bulk atmospheric stability.

286

287 *3.5 Station Data Appending*

288 Calculating the bulk atmospheric stability depends on the vertical profiles of potential
289 temperature and pressure. The bulk atmospheric stability is not representative of the valley
290 conditions when the radiosonde is released above the valley floor. For example, in Reno the
291 vertical extent of the missing data between the ASOS station on the valley floor and radiosonde
292 site is 174 m (see Table 1). Station data from the valley floor are pivotal to identify CAPs,
293 especially if the CAP is shallow (i.e., less than 200 m). Appending NWS maintained station data
294 to radiosondes ensures the entire vertical profile of the atmosphere in the valley is well
295 represented and is required to calculate a more accurate bulk stability to identify CAP events. In
296 addition, 10-m wind speed on the valley floor is crucial for classifying CAP events (e.g.,
297 classification method in Yu et al., (2017)). If the 10-m wind speed is not included in the vertical
298 profiles where the radiosonde is released above the valley floor, misclassifications of CAP events
299 are possible due to the increasing wind speed with height.

300 Appending surface station data to radiosonde observations in the western U.S. yields
301 better CAP classification results compared to methods that solely rely on radiosonde data (Green
302 et al., 2015, Pierce et al., 2019). Spokane, Elko and Reno have NWS maintained ASOS stations
303 on the valley floor with data spanning the entire study period; KSFF, KEKO and KRNO
304 respectively. These data are merged with the radiosonde datasets based on time stamps and the
305 data from surface stations are appended onto radiosonde observations, essentially adding a lower
306 elevation point to the vertical radiosonde record. The combined, surface station and radiosonde,
307 dataset was missing less than 5% of the data (i.e., radiosonde launch failure or maintenance on
308 NWS stations when observations led to missing data), therefore adding the station data did not
309 significantly reduce the data availability.

310 To evaluate the impact of appending the ASOS station data onto the radiosonde record, a
311 sensitivity analysis is conducted using the Medford radiosonde data. This analysis provides an
312 assessment for determining the effects of releasing radiosondes above the valley floor on
313 calculating a bulk atmosphere stability. Quantifying this impact is especially important for
314 locations where NWS maintained stations are absent (i.e., Riverton, Great Falls and Grand
315 Junction). The sensitivity analysis includes two parts. The first, calculates the impact of missing
316 vertical data on VHD and the second estimates the VHD errors associated with adding station
317 data from the valley floor onto the radiosonde record.

318 To calculate the impact of missing data on VHD, measurements in the lowest 205 m
319 AGL layer of the Medford radiosonde record are withheld to model a situation where the
320 radiosonde is released 205 m above the valley floor. Using this modeled missing data radiosonde
321 profile, a bulk atmospheric stability (VHD) is calculated for each radiosonde. When compared to
322 the VHD calculated using the full radiosonde record, the VHD calculated using the modeled
323 vertical profile with missing data quantifies the underestimation of bulk atmospheric stability.
324 This provides an estimate for the underestimated VHD in Riverton, Great Falls and Grand
325 Junction, where the station meteorology data on the valley floor are unavailable. The radiosonde
326 in Riverton is released 194 m above the valley, less than 205 m AGL, therefore this modeled
327 radiosonde profile from Medford provides the ‘worst case scenario’ estimate.

328 Next, to analyze the VHD errors associated with appending surface meteorology data
329 onto to radiosonde record another sensitivity test is done using the Medford radiosonde data. In
330 this analysis, the modeled vertical profile is similar to the case above (measurements in the
331 lowest 205 m AGL layer of the radiosonde record are withheld) but now a surface observation is
332 added onto the vertical record. This simulates adding the 10-m observations to the radiosonde
333 and another modeled VHD is calculated. Then the difference between the observed VHD and the
334 VHD calculated from appending surface station data onto the radiosonde record is calculated to
335 estimate the VHD errors. This provides insight into the impact of the vertical integration in the
336 VHD calculation (Equation 1) for the lowest level where the most stable layer is typically found
337 during CAPs (i.e., does appending surface meteorology data artificially increase the VHD).

338

339 4. Results

340 The overall objective of this paper is to develop a new classification method for
341 identifying CAP events in the western U.S. by analyzing previous classification methods and
342 exploring valley meteorology for each location (i.e., Columbia Basin, Truckee Meadows, Snake
343 River Basin, Rogue Valley, etc.). One goal of this new method is to create a CAP metric that can
344 be used in any location that allows for comparison across locations. The first step is to highlight
345 the importance of appending station data from the valley floor to radiosondes in locations where
346 the radiosondes are released from elevations above the valley floor (e.g., Reno, Elko, and
347 Spokane). The next step is to analyze the air pollution concentrations, bulk atmospheric stability
348 (VHD), 10-m wind speeds, and lapse rates to determine a framework for identifying the

349 meteorological processes that influence CAP events. Finally, results from the new method
350 described above in Section 3.4 are shown, including a comparison of the CAP prevalence across
351 12 cities in the western U.S. for 16 winters.

352

353 *4.1 Evaluation of Appending ASOS to Radiosonde Data*

354 To evaluate the impact of appending surface station data onto the radiosonde vertical
355 profiles the Medford site is used for a data withholding comparison of the appended vertical
356 profiles. When all soundings in Medford are considered to have a radiosonde launch elevation of
357 205 m AGL (withholding the data from the first 205 m above the ground), the modeled VHD is
358 1.47 MJ m⁻² lower than the observed VHD over the 16 winters. Thus, missing the lowest layer of
359 the atmosphere hinders the ability to classify a CAP. Misclassification of CAPs can hinder air
360 quality forecasting and has implications for residents residing in the lowest part of a valley. For
361 example, when stratifying the data withholding results by selecting only the soundings with
362 VHD values above the new CAP VHD threshold (VHD_{met} results shown in Section 4.3.4), the
363 modeled missing data VHD is 2.95 MJ m⁻² lower than the observed VHD. This indicates that
364 low-level temperature inversions occur near the surface and that the stable layer near the surface
365 impacts the VHD calculation.

366 Estimating the errors associated with the station data appending is necessary to
367 understand the impact on the calculated VHD. When forcing the vertical resolution of the first
368 two data points of the radiosonde record to be 205 m (i.e., simulating the case where surface
369 observations are appended onto the radiosonde record), the modeled VHD is 0.32 MJ m⁻² greater
370 than the observed VHD in Medford for all CAP soundings. The 12Z and 00Z soundings have a
371 modeled VHD increase of 0.43 and 0.07 MJ m⁻², respectively. These results indicate that
372 appending ASOS to radiosonde data is appropriate to extend the vertical profiles down to the
373 surface.

374 In this study, station data are appended onto the radiosonde record in three locations.
375 Table 2 shows the increased median and mean VHD when valley station data is appended to the
376 radiosondes. In Reno, Spokane, and Elko the overall median VHD increased 54.8%, 25.9%, and
377 20.7%, respectively, throughout the study period. The Reno radiosonde represents the largest
378 amount of missing data (174 m) and has a larger slope in the linear relationships between the two
379 VHDs than Elko and Spokane, confirming that it has the largest increase in VHD values. The

380 Table 2. **Data Appending Evaluation.** Mean, median, and standard deviation VHD values (MJ m^{-2}) for three
 381 locations (REV, LKN, OTX). *Radiosonde Only* - data provided by the radiosonde. *Appended Radiosonde* - ASOS
 382 data appended to the bottom of the radiosonde data. Slope and correlation for the regression between the two VHDs.

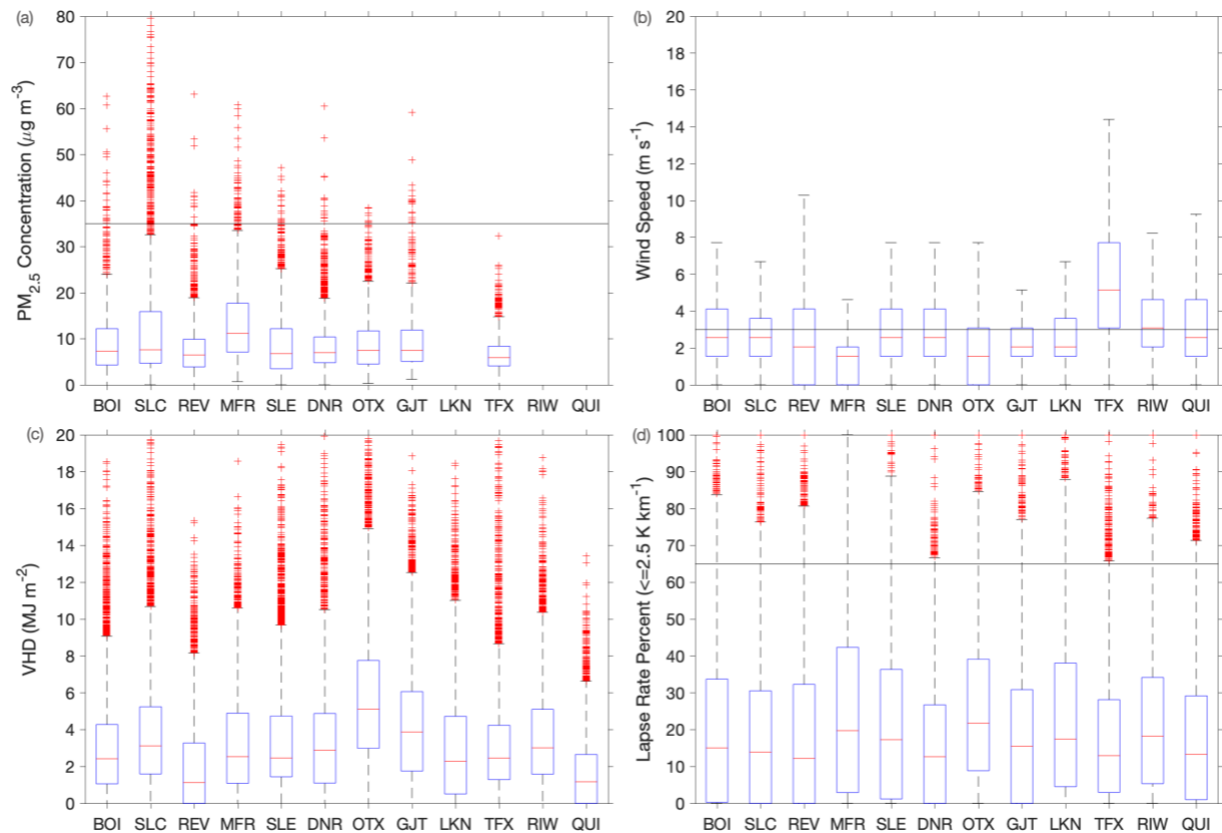
	Mean VHD (MJ m^{-2})	Median VHD (MJ m^{-2})	σ VHD (MJ m^{-2})	Correlation	Slope
REV					
Radiosonde Only	1.17	0.73	1.50		
Appended Radiosonde	1.98	1.13	2.55	0.968	1.691
OTX					
Radiosonde Only	4.58	4.05	3.40		
Appended Radiosonde	5.71	5.10	4.20	0.994	1.237
LKN					
Radiosonde Only	2.57	1.88	2.63		
Appended Radiosonde	3.10	2.27	3.15	0.997	1.199

383
 384 Elko radiosonde has the least amount of missing data near the surface (68 m) and has the
 385 smallest slope when the ASOS data are included in the vertical profile. More information on the
 386 correlation of appending ASOS data to radiosonde can be found in the supplement information.
 387 For Reno, Spokane, and Elko, all of the following results in this paper are calculated using
 388 vertical profiles with station data appended to the radiosonde vertical profile.

389
 390 *4.2 Statistics of wintertime meteorology and air quality*

391 Statistics of $\text{PM}_{2.5}$ concentrations, 10-m wind speed, VHD, and lapse rate percentages
 392 (i.e., percent of the lowest 1.5-km layer with a $\text{LR} \leq 2.5^\circ\text{C km}^{-1}$) from sounding data at 00Z and
 393 12Z for all locations over the study period are shown in Figure 2. These variables are key
 394 variables to identify CAPs in existing classification methods.

395 $\text{PM}_{2.5}$ concentrations are useful for identifying events (e.g., CAPs and wildfires) that
 396 contribute to poor air quality. Figure 2a shows that peak $\text{PM}_{2.5}$ concentrations are the highest in
 397 Salt Lake City, likely related to the anthropogenic air pollution emissions with a population
 398 greater than one million and industrial processes in the valley. Medford also experiences high
 399 pollution, relative to other locations in this study, despite having a lower population than Salt
 400 Lake City. The mean and median $\text{PM}_{2.5}$ concentrations are highest in Medford.



401
 402 **Figure 2. Box Plots for Oct-Mar from 2002-2018.** (a) PM_{2.5} concentrations line for 24-hr PM_{2.5}NAAQS, (b) 10-m
 403 wind speed line for VCP threshold, (c) VHD, and (d) percentage of lapse rates less than 2.5 K km⁻¹ in the lowest
 404 1500 m MSL line for DSL threshold. Median (red line), mean (box middle), 75th and 25th percentiles (box top and
 405 bottom), 1.5 times the interquartile (dashed lines), and outliers (red plus).

406 The 10-m wind speed shown in Figure 2b is required in the classification criteria used in
 407 Yu et al., (2017) for VCP and the new VHD_{met} developed in this paper. The median wind
 408 speeds are similar at all locations ranging from 2 m s⁻¹ to 3 m s⁻¹, except for Medford and Great
 409 Falls. Medford is the only location with a median 10-m wind speed less than 1 m s⁻¹, which is
 410 related to its local topography that creates orographic barriers to the flow. Medford lies in the
 411 Rogue Valley with mountains ~800 m AGL in all directions. The downstream mountains have a
 412 higher elevation than the upstream mountains, which is favorable for stagnation at the surface in
 413 the Rogue Valley due to the blocking effect. CAP erosion by turbulent mixing from above plays
 414 a minor role in deep valleys, which have complex wind regimes (Zängl 2005). Great Falls and
 415 Reno have the greatest overall 10-m wind speed which can be attributed to the local meteorology
 416 influenced by terrain. The upstream mountains in both locations have a higher elevation than the
 417 downstream mountains and are oriented North-South, promoting down-sloping wind events due
 418 to the West-East oriented jet stream typically associated with an incoming trough.

419 The VHD for each valley in Figure 2c suggests that the bulk stability varies with each
420 valley and is independent of PM_{2.5} concentrations (only when PM_{2.5} concentrations are compared
421 across all locations). Reno, Elko, Great Falls, and Quillayute have the lowest VHD values. In
422 arid locations, like Reno and Elko, the sensible heat flux can be an order of magnitude greater
423 than the latent heat flux (Albertson et al., 1995). Upward surface sensible heat flux during the
424 daytime tends to create rising parcels of air and enhance vertical mixing in the boundary layer
425 (Holmes et al., 2015). Quillayute is on the Pacific Northwest Coast and experiences frequent
426 synoptic systems during winter months and a lower VHD is expected, when compared to other
427 locations surrounded by mountains that act as barriers.

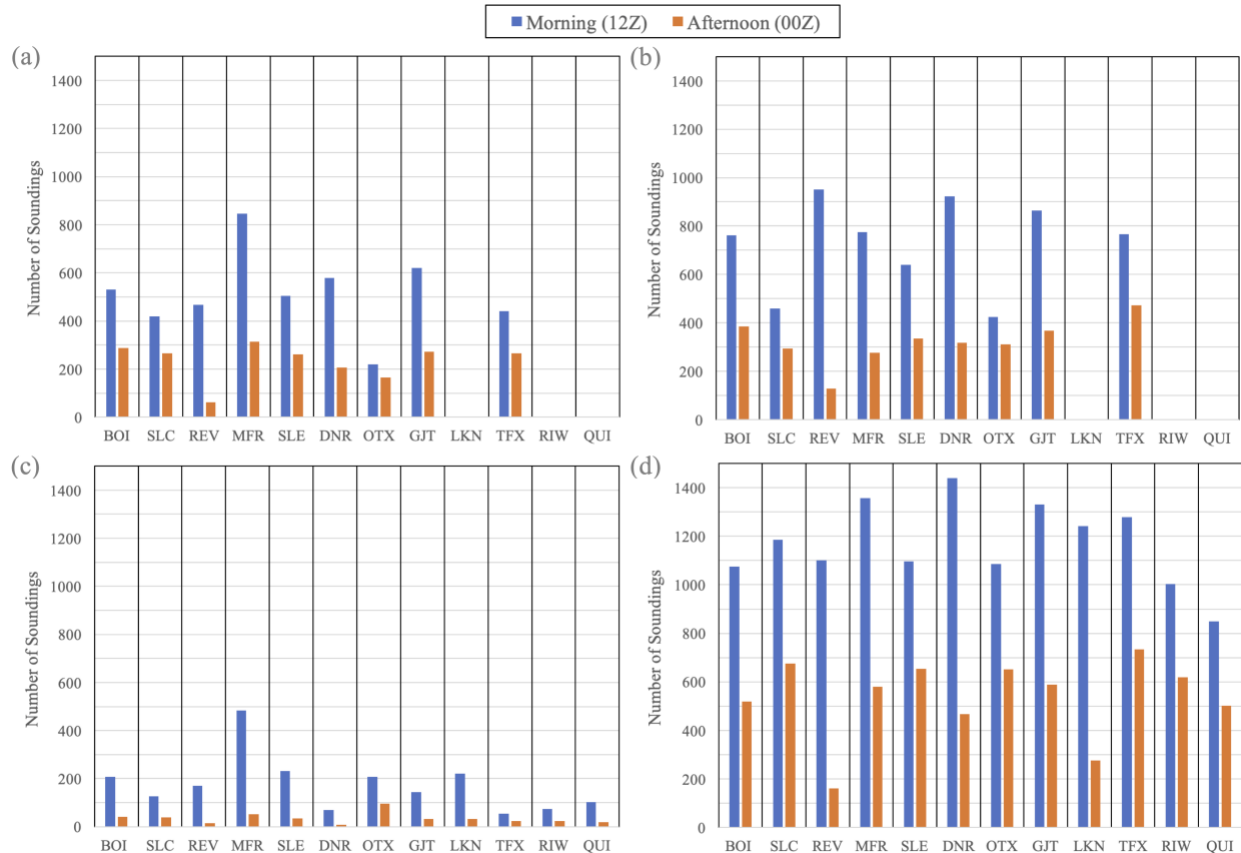
428 Lapse rate percentages can be used to quantify the presence of a deep temperature
429 inversion layer present near the surface. Medford and Spokane have the deepest layers of
430 temperature inversions (Figure 2d) over the time period with the 75th percentile reaching ~40%
431 for both locations. Denver and Quillayute have the lowest LR percentages and can be attributed
432 to the local meteorology (lee cyclogenesis and lack of downstream mountains for Denver and
433 active weather pattern for Quillayute). Denver lies on the front range of the Rockies, where polar
434 continental airmasses often influence meteorology and push the cold airmass against the
435 mountains. Quillayute lies on the coast of the Pacific Northwest, a common place for land falling
436 troughs in the wintertime.

437

438 *4.3 Cold Air Pool Classifications*

439 Figure 3 shows number of soundings that reach the thresholds for VHD_{17.5}, VHD₇₅,
440 VCP, and VHD_{met} at 12Z and 00Z. The number of days with potential persistent CAPs can be
441 inferred from Figure 3 by comparing the number of afternoon (00Z) sounding occurrences to
442 morning (12Z) occurrences. When the 00Z sounding threshold is met for any classification
443 method, a stable atmosphere is present and is likely persisting from the previous morning (12Z)
444 sounding. The 12Z soundings reached the CAP criteria more often than 00Z soundings in all four
445 methods due to the greater atmospheric stability in the lower levels in the morning. The locations
446 with a higher number of afternoon CAP occurrences implies that certain valleys may experience
447 more persistent CAP events (i.e., less afternoon mixing during such events).

448 Table 3 shows the VHD thresholds used in Figure 3 to determine the number of
449 soundings for CAP occurrences. Often, VHD_{17.5} threshold, based on Whiteman et al., (2014)



450

451 **Figure 3. CAP Occurrences for Oct-Mar from 2002-2018.** Number of CAP soundings for morning (12Z, blue)
 452 and afternoon (00Z, orange) sounding; 5,832 maximum soundings for each location. (a) VHD_17.5 based on
 453 Whiteman et al., (2014), (b) VHD_75 based on Pierce et al., (2019), (c) VCP based on Yu et al. (2017), and (d)
 454 VHD_met developed in this paper. *Note: Missing data for LKN, RIW and QUI due to lack of PM_{2.5} data.*

455 is greater than the VHD_75 threshold. The exception is Medford, where the 75th percentile of
 456 PM_{2.5} is greater than half of the NAAQS of 17.5 μg m⁻³, at 17.7 μg m⁻³ so the VHD_75 threshold
 457 is larger than the VHD_17.5 threshold. Figure 3 illustrates the differences in CAP behavior
 458 across 12 locations. For example, Great Falls has the greatest number of afternoon soundings
 459 reaching the VHD_75 threshold, implying that the afternoon mixing is frequently limited. In
 460 addition, more PCAP events are possible in Great Falls because of the decreased likelihood of
 461 mixing in the afternoon compared to other locations.

462 The results shown in Figure 3 using the four CAP classification methods highlight the
 463 ambiguity of these classification methods, where each method provides a significantly different
 464 number of CAP occurrences in each location. The number of CAP occurrences using the VHD
 465 thresholds based on PM_{2.5} values (VHD_17.5, VHD_75) are much higher than the number from
 466 the VCP method at each location. Another large difference comes from using air quality data

467 Table 3. **VHD Thresholds.** 75th percentile PM_{2.5} concentrations and VHD thresholds for 2002-2018 in 12 cities.
 468 VHD_{17.5}: mean VHD for 24-hr PM_{2.5} reaching half of the NAAQS (Whiteman et al., 2014), VHD₇₅: mean VHD
 469 for 24-hr PM_{2.5} exceeding the 75th percentile (Pierce et al., 2019), VHD_{met}: median VHD based on local
 470 meteorology, MALR VHD: mean VHD using idealized lapse rate, and Normalized VHD: normalized VHD greater
 471 than 1.0 indicates that lapse rates are less than the MALR. *Missing values indicate no PM_{2.5} monitors.*

Station ID	BOI	SLC	REV	MFR	SLE	DNR	OTX	GJT	LKN	TFX	RIW	QUI
PM_{2.5} 75th Percentile ($\mu\text{g m}^{-3}$)	12.2	15.9	9.9	17.7	12.2	10.4	11.7	11.9	--	8.4	--	--
VHD_{17.5} (MJ m^{-2})	5.94	7.49	5.77	5.62	6.95	6.43	10.19	7.56	--	6.06	--	--
VHD₇₅ (MJ m^{-2})	4.92	7.22	4.04	5.93	6.14	5.26	8.36	6.57	--	4.65	--	--
VHD_{met} (MJ m^{-2})	4.03	4.40	3.49	3.92	3.96	4.12	6.88	5.23	4.41	3.97	4.71	2.72
MALR VHD (MJ m^{-2})	2.13	2.80	1.46	1.50	1.73	2.73	3.41	3.37	1.80	2.32	2.34	1.79
Normalized VHD	2.00	1.59	2.60	2.54	2.38	1.57	2.09	1.60	2.69	1.58	2.13	1.51

472 versus meteorology data to establish a VHD threshold. For example, Great Falls has a greater
 473 number of CAPs than Medford based on the VHD_{met} threshold (Great Falls n=1807 and
 474 Medford n=1144) while Medford has a greater number of CAPs based on the VCP criteria (Great
 475 Falls n=77 and Medford n=534). Therefore, the CAP classifications differ significantly when
 476 applying these criteria to different locations, even with similar synoptic meteorology. These
 477 differences will be highlighted in the following subsections.

478
 479 **4.3.1 VHD based on PM_{2.5} NAAQS (VHD_{17.5})**

480 For all locations except Medford, VHD_{17.5} identified fewer CAP soundings than
 481 VHD₇₅ since fewer locations have PM_{2.5} concentrations greater than 17.5 $\mu\text{g m}^{-3}$. For the 12Z
 482 sounding observations, most locations reach 400-600 sounding occurrences (out of a possible
 483 2,800) during the study period. This suggests that ~20% of the mornings in the Intermountain
 484 West experience stable conditions, while less than ~10% of the afternoons experience stable
 485 conditions. The VHD_{17.5} thresholds in Table 3 are rather high, especially for Spokane, Salt
 486 Lake City and Grand Junction, which partly explains why there are fewer sounding occurrences
 487 despite previous studies that found an abundance of CAPs in these locations (Green et al., 2015;
 488 Whiteman et al., 2014; Yu et al., 2017).

489 To investigate this further the VHD thresholds from SLC can be used. The VHD_17.5
490 threshold in Table 3 for Salt Lake City, 7.49 MJ m^{-2} , is larger than the VHD threshold calculated
491 in Whiteman et al., (2014), 4.04 MJ m^{-2} . There are two possible explanations for this. The first, is
492 that in this study the sounding data does not have a fine scale vertical resolution (i.e., the
493 radiosonde data were not interpolated to 10-m resolution intervals) and the integration height
494 here was based on an average ridge height of 2439 m (instead of 2200 m). The second hypothesis
495 is that $\text{PM}_{2.5}$ concentrations show a decreasing trend in the U.S. in recent years, thus requiring a
496 higher VHD value for days with $\text{PM}_{2.5}$ concentrations larger than half of the NAAQS standard.
497

498 **4.3.2 VHD using 75th Percentile $\text{PM}_{2.5}$ (VHD_75)**

499 The 75th percentile $\text{PM}_{2.5}$ concentrations vary among the different valleys (Table 3).
500 Reno, Denver and Great Falls have the lowest $\text{PM}_{2.5}$ concentrations, which is expected because
501 the 10-m wind speed for these locations is greater (Figure 2b) than the other locations. Greater
502 wind speed near the surface is indicative of more vertical mixing and dispersion of air pollutants
503 near the surface, reducing the overall $\text{PM}_{2.5}$ concentrations. Medford has the highest 75th
504 percentile $\text{PM}_{2.5}$ concentration along with the lowest 10-m wind speed. The data in Table 3
505 coincides with data presented in Figure 2, where there is a negative relationship between wind
506 speed and $\text{PM}_{2.5}$ and a positive relationship between $\text{PM}_{2.5}$ and VHD.

507 In locations where $\text{PM}_{2.5}$ concentrations during the months from October to March are
508 low (i.e., Reno and Great Falls), the mean VHD thresholds are low as well. This indicates that
509 $\text{PM}_{2.5}$ concentrations that are considered to represent polluted days in Reno and Great Falls
510 require lower bulk atmospheric stability than other locations. The opposite is true for Salt Lake
511 City and Spokane, where a strong and/or deep stably stratified layer of atmosphere, indicated by
512 a higher VHD, are required to have polluted days (Table 3). Implying that VHD thresholds for
513 CAP classification based on air quality makes the comparison across locations ambiguous
514 because local emissions can have a large impact on the results.

515 Figure 3d shows the number of sounding occurrences that reach the VHD_75 threshold.
516 Reno has the least amount of afternoon soundings reaching the VHD_75 threshold, indicating
517 that efficient afternoon mixing occurs and implies that persistent CAPs are less frequent than
518 other locations. However, Reno has the greatest number of diurnal CAPs when compared to
519 other locations, suggesting effective radiational warming during the early morning hours. In

520 Table 3, the VHD_75 for Reno is the lowest, but this value is higher than the majority of the
521 afternoon soundings. Salt Lake City and Spokane have few morning CAP occurrences but high
522 afternoon occurrences relative to the number of morning CAPs, likely due to a higher VHD_75
523 threshold value, and also indicates an increased presence of persistent CAPs in both locations.
524

525 **4.3.3 Valley Cold Pool (VCP)**

526 The CAP sounding numbers identified using the VCP method proposed by Yu et al.,
527 (2017) are shown in Figure 3c. Afternoon (00Z) soundings in Spokane reached the VCP criteria
528 for 31.5% of the total soundings (n=302), while Denver 00Z soundings represent 11.5% (Figure
529 3c). This suggests that afternoon mixing is more likely in Denver while suppressed mixing
530 occurs in Spokane, and other locations. Figure 3c shows that nocturnal inversions are common
531 and dominant in the western U.S., which aligns with results based on the other CAP
532 classification methods. In addition, Figure 3c shows a significant number of mornings with VCP
533 criteria being met, while fewer afternoon soundings meeting the VCP criteria. The exceptions are
534 Great Falls, Riverton and Quillayute which experience greater 10-m wind speed (Figure 2b), thus
535 not meeting the VCP wind speed criteria of less than 3 m s^{-1} in the morning as well.

536 Medford total and morning VCP occurrences are greater than other locations by more
537 than 200 sounding occurrences (n=534). The number of afternoon VCP occurrences in Medford
538 is similar to other locations, possibly indicating the morning VCP occurrence could be due to
539 valley meteorological differences when compared to other locations. 10-m wind speeds in
540 Medford are low, with 75th percentile wind speeds below the VCP threshold of 3 m s^{-1} , and
541 deeper stable layers are observed more frequently in the morning (Figure 2b & 2d). VCP
542 occurrences are strongly related to the deep stable criteria developed by Wolyn and Mckee
543 (1989), apart from 10-m wind speed criteria discussed in Yu et al., (2017).
544

545 **4.3.4 VHD with Meteorological Thresholds (VHD_met)**

546 Identifying days with high surface pressure and decreased near-surface wind speed
547 allows for identifying stagnant weather conditions associated with CAP events. Defining a VHD
548 threshold that depends on physical variables that characterize the CAP provides a consistent
549 method of classifying such events across valleys or locations. The median VHD_met thresholds
550 for the 12 locations are similar, with most locations in a range of $4 \pm 1 \text{ MJ m}^{-2}$ (Table 3).

551 Spokane, Grand Junction, and Quillayute are outside this range with VHD thresholds of 6.88,
552 5.23 and 2.72 MJ m⁻², respectively.

553 This new method for classifying CAPs is independent of air pollution, thus there is less
554 variability in the VHD_met thresholds (Table 3) and the number of CAPs (Figure 3d) across the
555 12 locations compared to the VHD_17.5 and VHD_75 methods. The number of soundings that
556 meet or exceed the VHD_met threshold in each location are similar (Figure 3d) with a mean of
557 1706 soundings and a standard deviation of 241 soundings, when averaged across all locations.
558 As expected, the morning (12Z) sounding frequently exceeds the VHD_met threshold due to
559 decreased vertical mixing during the overnight and early morning hours, with fewer CAP
560 occurrences in the afternoon (00Z) soundings. Salt Lake City, Spokane, and Great Falls have the
561 greatest number soundings over the VHD_met thresholds in the 00Z soundings, indicating that
562 persistent CAPs possibly persist through the diurnal cycle. Reno and Elko have the lowest
563 number of 00Z soundings reaching their VHD_met thresholds, indicating the typical diurnal
564 cycles likely inhibit persistent CAP formation in these locations.

565

566 *4.4 Persistent Cold Air Pool (PCAP)*

567 A PCAP is defined as a CAP that lasts for 3 or more consecutive twice-daily soundings (based
568 on the definition in Whiteman et al., (2014)). Meaning a PCAP is a CAP that persists for more
569 than one diel cycle, this same definition is used here and aligns with previous research (e.g., Yu
570 et al., (2017) and Lareau et al., (2013)). PCAPs have significant health impacts because the CAP
571 persists through the afternoon and leads to increasing pollutant concentrations over long periods
572 of time. The number of PCAPs over the duration of this study varies significantly depending on
573 the location and the CAP classification method (Figure 4). Typically, locations that are farther
574 south and/or have an absence of downwind mountains observe fewer PCAPs, for all methods.
575 The variability in the number of PCAPs identified by the different methods further illustrates the
576 need for a universal classification method. The mean PCAP length determined by each method is
577 shown in Figure 4b. The mean PCAP lengths between VHD_75, VHD_17.5, and VHD_met are
578 similar, complementing previous research that synoptic meteorology influences PCAPs (Lareau
579 et al., 2013; Green et al., 2015; Yu et al., 2017). However, there are subtle differences in PCAP
580 length for each method. Where the VHD_met threshold method likely captures the PCAP length
581 more appropriately because it is based on synoptic meteorology and does not rely on air quality



582

583 Figure 4. **PCAP Characteristics for Oct-Mar from 2002-2018.** (a) Total number of PCAPs based on VHD_75
 584 from Whiteman et al., (2014), VHD_75 from Pierce et al., (2019), VCP from Yu et al., (2017), and the new
 585 VHD_met method. (b) Length of PCAPs in days; mean (bars), standard deviation (whiskers), median (dot), and
 586 maximum (square).

587 to establish a CAP threshold.

588 PCAP length changes with the method used, often varying by up to one day. The
 589 majority of the PCAP lengths for all locations are 4-6 consecutive soundings, or 2-3 days. Since
 590 PM_{2.5} varies from year to year, VHD_17.5 may not adequately identify PCAP events over
 591 decades. The 75th percentile PM_{2.5} concentration is less than half of the NAAQS at most
 592 locations, with the exception of Medford. Further, PM_{2.5} data is not available in Elko, Riverton,
 593 and Quillayute, complicating the classification of PCAPs in those locations. When comparing
 594 results of the novel method (VHD_met) to the previous methods, the length of PCAPs are

595 comparable, especially in Reno, Salt Lake City, Denver and Boise. When disregarding the
596 method used by Yu et al., (2017), variability in the three methods is limited and indicates that the
597 novel method can be useful for determining PCAP duration.

598

599 **4.4.1 VHD_17.5 (Whiteman et al., 2014)**

600 When using the VHD_17.5 threshold to determine the onset, duration, and breakup of
601 PCAPs, most locations observe 80-100 PCAPs (e.g., total number of PCAPs from 2002-2018)
602 with Reno, Denver and Great Falls having the least number of PCAPs (Figure 4a). Medford,
603 Spokane, and Grand Junction observe up to 7 PCAPs per winter on average. Medford has the
604 highest PM_{2.5} concentrations on average while Spokane and Grand Junction have the greatest
605 depth of integration, which may explain why these locations experience more PCAPs than other
606 locations. Reno experiences the least number of PCAPs during the study period, this is attributed
607 to fewer afternoon (00Z) soundings reaching the VHD_17.5 threshold (Figure 3a). Figure 4b
608 shows that the PCAP length from VHD_17.5 varies only by a couple of days at most between all
609 locations. Maximum PCAP lengths are not similar when comparing across all locations. This
610 indicates that the local valley meteorology influences PCAP events, which is further discussed in
611 the Supplemental Information.

612

613 **4.4.2 VHD_75 (Pierce et al., 2019)**

614 The total number of PCAPs increases using the VHD_75 method compared to the
615 VHD_17.5 method for all locations, with the exception of Medford. The number of PCAPs per
616 winter for most locations is approximately 7, with Spokane, Grand Junction and Great Falls
617 nearing 9 PCAPs per winter. Reno still experiences the least amount of PCAPs, even with the
618 lower VHD_75 threshold. In locations where the 75th percentile PM_{2.5} concentration is close to
619 17.5 µg m⁻³, the difference between the number of PCAPs using VHD_17.5 and VHD_75 is
620 minimal (i.e., Medford and Salt Lake). Great Falls, Denver, and Reno have the lowest 75th
621 percentile PM_{2.5} concentrations and thus have significantly more PCAPs with VHD_75 than
622 VHD_17.5 since the air pollution concentration threshold is lower using VHD_75 (i.e., requiring
623 a lower VHD threshold on days when the 75th percentile of PM_{2.5} is observed).

624

625 **4.4.3 VCP (Yu et al., 2017)**

626 Very few PCAPs are observed using the VCP method, likely due the absence of DSLs
627 during PCAPs that maintain a depth of 975 m (65% of the lowest 1500 m AGL layer), especially
628 during afternoon hours. Based on the VCP threshold, Boise and Medford have the greatest
629 number of PCAPs, 13 and 16, respectively over the study period, far fewer than other methods.
630 Other locations often have fewer than 10 PCAPs total, implying that PCAPs occur in most
631 valleys once or twice every other year when using VCP to classify PCAPs.

632 When the lapse rate percentage of the lower 1500 m AGL is lowered to 30-40% (500-600
633 m layer depth AGL), the number of PCAPs in each location is comparable to the other methods
634 discussed in this paper. Differences lie in the average length of the PCAPs when compared to the
635 other methods. For example, when the lapse rate percentage is maintained at 65%, the average
636 PCAP length is anywhere between 3-4 consecutive soundings. However, when the lapse rate
637 percentage is decreased to ~35%, the average PCAP length increases but is still less than the
638 average PCAP length calculated using the other methods. PCAP length using this method are
639 expected to be less than other methods because of the DSL requirement. PCAPs typically change
640 depth over the duration of a single event and using a criterion dependent on depth filters out
641 shallow stable layers below the ridge height.

642

643 **4.4.4 VHD_met**

644 The total number of PCAPs is the greatest for the new meteorological classification
645 (VHD_met) method (red bars in Figure 4). Since this method relies on synoptic meteorology,
646 some conformity across all locations can be observed. Meaning that the results across locations
647 are more similar using VHD_met, compared to the VHD based on air pollution, because the
648 large-scale synoptic conditions occur over the entire western U.S. impacting multiple locations at
649 the same time. When comparing the number of PCAPs in Elko, Riverton, and Quillayute, to the
650 number of PCAPs in other locations with similar climates (e.g., Spokane, Reno) using this
651 method they are now comparable. Elko and Reno have the lowest number of PCAPs, while
652 locations farther north typically experience more PCAPs. Quillayute observed the greatest
653 number of PCAPs, likely due to a low VHD_met threshold being easily reached during stagnant
654 periods and/or elevated inversions, which can also be met when marine boundary layers are
655 present. Additional investigation is required to separate the CAP events over mountains and
656 marine ABLs using this method.

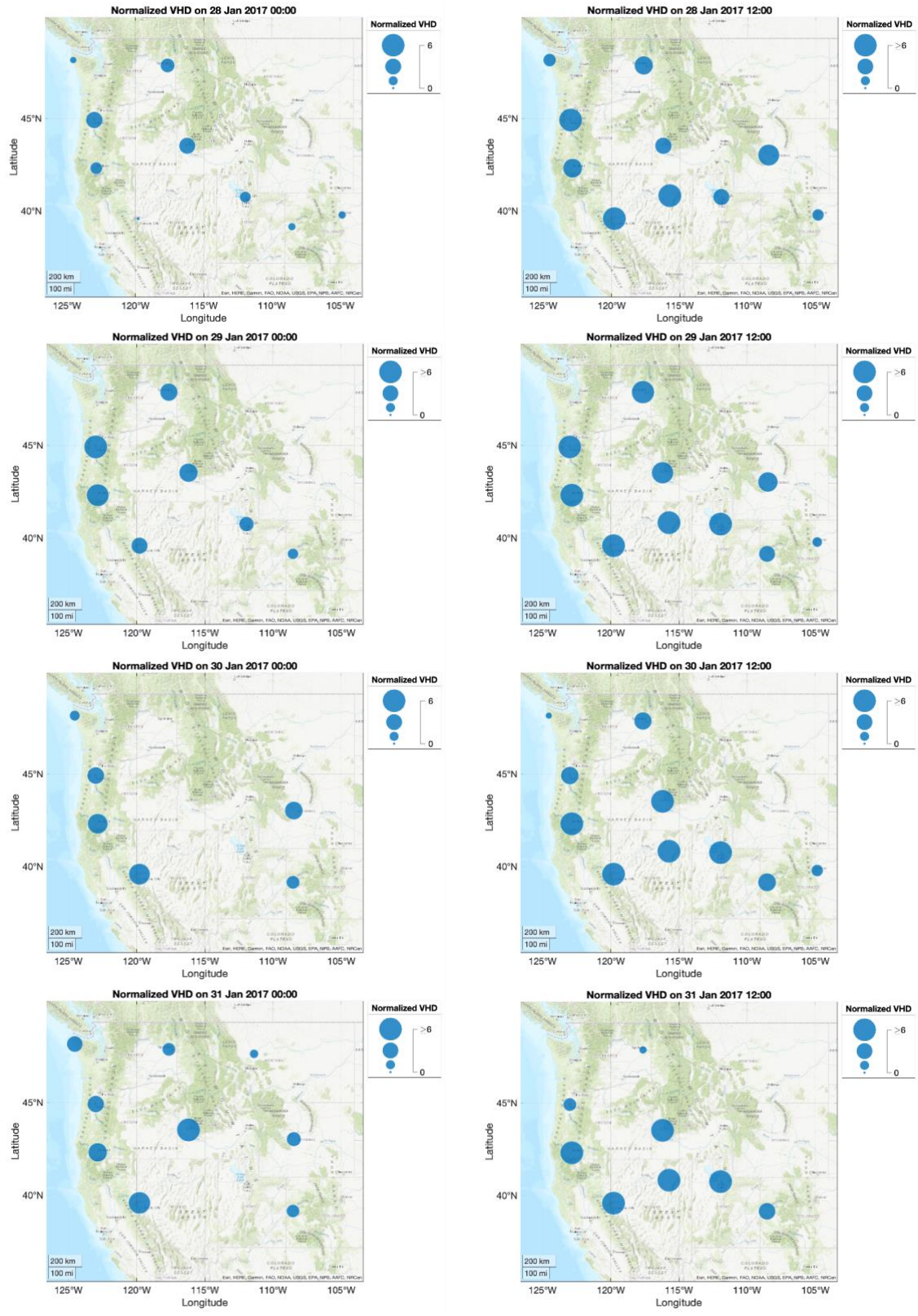
657

658 *4.5 Normalized VHD for Comparison Across Locations*

659 To create a CAP classification metric that is comparable across multiple locations, the
660 MALR VHD is used to normalize the VHD calculated from each radiosonde. Because the
661 physical interpretation of the VHD magnitude varies across locations, the VHD normalized with
662 an idealized MALR VHD provides a unitless VHD with a uniform scale for comparison. This
663 idealized profile uses the MALR to calculate an idealized VHD. The MALR VHD is location
664 specific and changes depending on the depth of the valley. For example, Medford has a mean
665 MALR VHD of 1.5 MJ m^{-2} with a standard deviation of less than 0.2 MJ m^{-2} , close to values
666 reported in Whiteman et al., (2014) for Salt Lake City. Grand Junction has a MALR VHD of
667 3.37 MJ m^{-2} with a standard deviation of 0.3 MJ m^{-2} . The valley depth in Medford is lower than
668 Grand Junction (438 m difference), resulting in a larger MALR VHD (i.e., deeper integration
669 heights increase the MALR VHD). Locations with greater integration depth (e.g., Spokane depth
670 is $\sim 1250 \text{ m AGL}$) have a greater MALR VHD because the integration includes more data points
671 and those data points have a higher vertical resolution than at lower altitudes. When comparing
672 valley integration depth to the MALR VHD they are correlated with an r^2 of 0.85, as integration
673 increases, the MALR VHD also increases. Once the normalized VHD values are obtained for
674 each radiosonde the new CAP classification method is applied at each location to calculate a new
675 normalized VHD_met threshold (Normalized VHD in Table 3).

676 Using a standard MALR of $0.0065^\circ\text{C m}^{-1}$, the MALR VHD is a general VHD value that
677 represents a normal stability for a standard atmosphere without the presence of a CAP.
678 Therefore, normalized VHD values greater than 1.0 for any radiosonde indicate a more stable
679 boundary layer. The normalized VHD thresholds calculated for each location range from 1.51 in
680 Quillayute to 2.60 in Reno and are shown in Table 3. Places with climatologically higher VHD
681 (Figure 2c), Spokane and Grand Junction, have normalized VHD values of 2.09 and 1.6,
682 respectively, which are comparable to the normalized VHD thresholds in the other locations.
683 When the normalized VHD is greater than the threshold values listed in Table 3, there is a CAP
684 (i.e., diurnal or persistent) and when three consecutive soundings reach this threshold, a PCAP is
685 identified.

686 The normalized VHD enables comparisons across locations. It can be used to identify
687 CAP events over large spatial scales and to compare the duration and timing of the events across



688
689
690
691

Figure 5. **Normalized VHD Values for CAPs.** Normalized VHD in each location for soundings that were above the normalized VHD threshold value, indicating a CAP for 28-31 January 2017 UTC. (Left) Afternoon soundings, 00Z. (Right) Morning soundings, 12Z. Consecutive soundings indicate a PCAPs.

692 locations. For example, Figure 5 shows the spatial distribution of the normalized VHD for
693 soundings over the CAP threshold (Table 3) for four days in January 2017. It shows that large
694 scale processes (synoptic meteorology) cause CAP formation in several valleys across the
695 western U.S., where six to ten locations in each plot have a CAP. Additionally, the presence of
696 PCAPs can be seen in eight locations over the four-day period (Quillayute, Medford, Salem,
697 Spokane, Boise, Reno, Salt Lake City, and Grand Junction).

698

699 5. Discussion

700 CAP formation in the mountainous areas over the western U.S. occurs when there is a
701 500 hPa ridge system and surface cold anomaly based on climatology analysis. In previous
702 studies, the two CAP classification criteria from literature were applied to the SLV, but only
703 broadly to other valleys (e.g., Green et al., (2015); Yu et al., (2017)). Large scale studies have
704 shown that CAPs occur in other valleys; however, field campaigns outside of the SLV and
705 Columbia River Basin are rare and potentially inhibits the ability to understand the physical
706 processes that influence CAPs in other valleys. Whiteman et al., (2001) found that PCAPs in the
707 lower Columbia River Basin persisted for a median duration of 28.5 hours from 1989-1999 using
708 observational station data. Local topography like upwind/downwind mountain heights, valley
709 shape and predominant wind direction influence CAP events. Wind roses during CAP events and
710 non-CAP events above the average ridge height provides insights to why some locations
711 experience deeper stable layers, greater bulk stability and possibly the duration of a CAP event
712 (see Supplemental Information for wind roses). For example, Medford typically experiences a
713 light northerly wind at the surface and a SE wind at the average ridge height during the winter
714 months and especially during PCAPs.

715 Persistent CAPs lasting longer than one diurnal cycle may be partially enhanced by
716 radiative effects, but are predominantly forced by large-scale subsidence and/or mid-level warm
717 air advection (Wolyn and McKee 1989; Whiteman et al., 1999, 2001; Zhong et al., 2001; Zängl
718 2005; Hoggarth et al., 2006; Reeves and Stensrud 2009). This is especially evident in Figure 4a
719 with all locations experiencing a similar number of PCAPs, their proximity to large-scale
720 subsidence can be attributed to this. The predominance of large-scale patterns that lead to these
721 events are important to understand. The criteria discussed in this paper are mostly associated
722 with large-scale meteorological patterns that contribute to CAPs. It should be noted that local

723 meteorology is important for the duration and strength of the CAP, as seen in Medford, OR and
724 Reno, NV, where deep CAPs and more shallow CAPs are dominant. Brief discussions of the
725 local meteorological conditions at each location are given in the Supplemental Information to
726 illustrate the influence of these factors on CAP events.

727 Snow impacts influence CAP behavior and can extend PCAP length. Increased surface
728 albedo due to snow cover impacts the surface energy balance and causes more of the incoming
729 solar radiation to be reflected from the surface. Therefore, there is less net radiation at the surface
730 and a lower surface sensible heat flux to transfer heat from the ground to the boundary layer,
731 which dampens the mixing and can lead to increased PM_{2.5} concentrations. Green et al., (2015)
732 found that snow-covered CAP days (22%) were nearly four times greater than no snow-covered
733 CAP days (5.3%). Additional information about the snow impacts in specific locations are
734 included in the local meteorological discussions in the Supplemental Information.

735

736 6. Summary

737 CAPs studies can be biased when using radiosonde data that comes from radiosonde
738 launches released above the valley floor because the data does not include the lowest portion of
739 the atmosphere where a strong stable layer can be present. Appending ASOS meteorological data
740 on the valley floor to radiosonde data resulted in a more representative VHD to quantify the
741 stability of the atmosphere. Stability can be underestimated by as much as 50% for locations
742 where the radiosonde is released >150 m above the valley floor. More CAP events are identified
743 when accounting for the vertical structure of the entire valley depth.

744 This paper uses four methods (VHD_{17.5}, VHD₇₅, VCP, and VHD_{met}) to classify
745 CAP events in the western U.S. using observational data from radiosondes and ASOS data where
746 needed. The new metric introduced in this paper (VHD_{met}) suggests that criteria related to
747 synoptic meteorology results in similar CAP VHD threshold values across the western U.S.,
748 especially where valley depths are similar. Previous classification methods (VHD_{17.5} and
749 VHD₇₅) based on air quality have CAP VHD threshold values that vary significantly by
750 location and are influenced by air pollution emissions. Calm winds near the surface, high
751 pressure, mid-level warming, higher RH, and snow cover are characteristics of a PCAP,
752 regardless of population. While air pollution increases during a PCAP, the increased PM_{2.5}
753 concentrations are valley specific and have the potential to change significantly across decades.

754 The new CAP classification metric provides a method for classifying PCAPs in any location that
755 has vertical profiles of meteorology data. In addition, this new method provides a way for health
756 officials, emergency managers, and government officials to determine when CAP events are
757 present to further understand atmospheric chemistry, adverse health impacts, and more during
758 these events. Additional valley specific meteorology needs further investigation including
759 drainage flows, differences in why diurnal CAPs do not evolve into persistent CAPs, PCAPs that
760 are resilient, and vertical profiles of turbulent fluxes to understand boundary layer mixing.

761

762 **Acknowledgements**

763 The authors would like to thank former University of Nevada, Reno graduate students Dr.
764 S. Marcela Loría-Salazar and KC King for their assistance with troubleshooting and developing
765 python codes to process the large amounts of radiosonde data used in this study.

766

767 **References**

- 768 Albertson, J.D., Parlange, M.B., Katul, G.G., Chu, C.-R., Stricker, H., & Tyler, S., 1995.
769 Sensible heat flux from arid regions: A simple flux-variance method. *Water Resources*
770 *Research* **31**, 969–973. <https://doi.org/10.1029/94WR02978>
- 771 Baasandorj, M., Hoch, S. W., Bares, R., Lin, J. C., Brown, S. S., Millet, D. B., Martin, R., Kelly,
772 K., Zarzana, K. J., Whiteman, C. D., Dube, W. P., Tonnesen, G., Jaramillo, I. C., & Sohl,
773 J. 2017. Coupling between chemical and meteorological processes under persistent cold-
774 air pool conditions: Evolution of wintertime PM_{2.5} pollution events and N₂O₅
775 observations in Utah’s Salt Lake Valley. *Environmental Science and Technology* **51**,
776 5941–5950.
- 777 Clay, K. & Muller, N., 2019. Recent Increases in Air Pollution: Evidence and Implications for
778 Mortality (No. w26381). National Bureau of Economic Research, Cambridge, MA.
779 <https://doi.org/10.3386/w26381>
- 780 Deardorff, J.W., 1970. Convective velocity and temperature scales for the unstable planetary
781 boundary layer and for Rayleigh convection. *Journal of Atmospheric Science*. **27**, 1211–
782 1213. [https://doi.org/10.1175/1520-0469\(1970\)027<1211:CVATSF>2.0.CO;2](https://doi.org/10.1175/1520-0469(1970)027<1211:CVATSF>2.0.CO;2)
- 783 Franchin, A., Fibiger, D. L., Goldberger, L., McDuffie, E. E., Moravek, A., Womack, C. C.,
784 Crosman, E. T., Docherty, K. ^[1]_{SEP}S., Dube, W. P., Hoch, S. W., Lee, B. H., Long, R.,
785 Murphy, J. G., Thornton, J. A., Brown, S. S., Baasandorj, M. & Middlebrook, A. M.
786 2018. Airborne and ground-based observations of ammonium-nitrate-dominated aerosols
787 in a shallow boundary layer during intense winter pollution episodes in northern Utah.
788 *Atmospheric Chemistry and Physics* **18**, 17259–17276. ^[1]_{SEP}
- 789 Green, M.C., Chow, J.C., Watson, J.G., Dick, K., & Inouye, D., 2015. Effects of snow cover and
790 atmospheric stability on winter PM_{2.5} concentrations in western U.S. valleys. *Journal of*
791 *Applied Meteorology and Climatology*. **54**, 1191–1201. [https://doi.org/10.1175/JAMC-D-](https://doi.org/10.1175/JAMC-D-14-0191.1)
792 14-0191.1
- 793 Hoggarth, A.M., Reeves, H.D., & Lin, Y.-L., 2006. Formation and Maintenance Mechanisms of
794 the Stable Layer over the Po Valley during MAP IOP-8. *Monthly Weather Review* **134**,
795 3336–3354. <https://doi.org/10.1175/MWR3251.1>
- 796 Holmes, H.A., Sriramasamudram, J.K., Pardyjak, E.R., & Whiteman, C.D., 2015. Turbulent

797 fluxes and pollutant mixing during wintertime air pollution episodes in complex terrain.
798 *Environmental Science and Technology*. **49**, 13206–13214.
799 <https://doi.org/10.1021/acs.est.5b02616>

800 Horel, J., Splitt, M., Dunn, L., Pechmann, J., White, B., Ciliberti, C., Lazarus, S., Slemmer, J.,
801 Zaff, D., & Burks, J. 2002 Mesowest: Cooperative mesonets in the western United States.
802 *Bulletin of the American Meteorological Society* **83**, 211-226.

803 Ivey, C. E., Balachandran, S., Colgan, S., Hu, Y. & Holmes, H. A. 2019. Investigating fine
804 particulate matter sources in Salt Lake City during persistent cold air pool events.
805 *Atmospheric Environment* **213**, 568–578 (2019). ^[1]_{SEP}

806 Jemmett-Smith, B.C., Ross, A.N., Sheridan, P.F., Hughes, J.K., & Vosper, S.B., 2019. A case-
807 study of cold-air pool evolution in hilly terrain using field measurements from COLPEX.
808 *Quarterly Journal of the Royal Meteorological Society* **145**, 1290–1306.
809 <https://doi.org/10.1002/qj.3499>

810 Lareau, N.P., Crosman, E., Whiteman, C.D., Horel, J.D., Hoch, S.W., Brown, W.O.J., & Horst,
811 T.W., 2013. The Persistent Cold-Air Pool Study. *Bulletin of the American Meteorological*
812 *Society* **94**, 51–63.

813 Lareau, N.P. & Horel, J.D., 2015a. Dynamically Induced Displacements of a Persistent Cold-Air
814 Pool. *Boundary-Layer Meteorology* **154**, 291–316.

815 Lareau, N.P. & Horel, J.D., 2015b. Turbulent Erosion of Persistent Cold-Air Pools: Numerical
816 Simulations. *Journal of the Atmospheric Sciences* **72**, 19.

817 NOAA, 1976: U.S. Standard Atmosphere, 1976. NOAA Tech. Rep. S/T 76-1562, National
818 Oceanic and Atmospheric Administration, Washington, D.C. [Available online at
819 <https://ntrs.nasa.gov/archive/nasa/casi.ntrs.nasa.gov/19770009539.pdf>].

820 Pierce, A.M., Loría-Salazar, S.M., Holmes, H.A., & Gustin, M.S., 2019. Investigating horizontal
821 and vertical pollution gradients in the atmosphere associated with an urban location in
822 complex terrain, Reno, Nevada, USA. *Atmospheric Environment* **196**, 103–117.
823 <https://doi.org/10.1016/j.atmosenv.2018.09.063>

824 Pope III, C.A., 1991. Respiratory Hospital Admissions Associated with PM10 Pollution in Utah,
825 Salt Lake, and Cache Valleys. *Archives of Environmental Health: An International*
826 *Journal* **46**, 90–97. <https://doi.org/10.1080/00039896.1991.9937434>

827 Pope III, C.A., Muhlestein, J.B., May, H.T., Renlund, D.G., Anderson, J.L., & Horne, B.D.,

828 2006. Ischemic heart disease events triggered by short-term exposure to fine particulate
829 air pollution. *Circulation* **114**, 2443–2448.

830 Reeves, H.D. & Stensrud, D.J., 2009. Synoptic-Scale Flow and Valley Cold Pool Evolution in
831 the Western United States. *Weather and Forecasting* **24**, 1625–1643.

832 Shin, S.-H. & Ha, K.-J., 2009. Implementation of turbulent mixing over a stratocumulus-topped
833 boundary layer and its impact in a GCM. *Advances in Atmospheric Sciences* **26**, 995–
834 1004. <https://doi.org/10.1007/s00376-009-8145-0>

835 Silcox, G.D., Kelly, K.E., Crosman, E.T., Whiteman, C.D., & Allen, B.L., 2012. Wintertime
836 PM_{2.5} concentrations during persistent, multi-day cold-air pools in a mountain valley.
837 *Atmospheric Environment* **46**, 17–24.

838 Sun, X. & Holmes, H. Surface turbulent fluxes during persistent cold-air pool events in the Salt
839 Lake Valley, Utah. Part I: Observations. *Journal of Applied Meteorology and*
840 *Climatology* **58**, 2553–2568 (2019).

841 VanReken, T. M., Dhammapala, R. S., Jobson, B. T., Bottenus, C. L., VanderSchelden, G. S.,
842 Kaspari, S. D., Gao, Z., Zhu, Q., Lamb, B. K., Liu, H., & Johnston, J. 2017. Role of
843 persistent low-level clouds in mitigating air quality impacts of wintertime cold pool
844 conditions. *Atmospheric Environment* **154**, 236–246. ^[1]_{SEP}

845 Whiteman, C.D., Bian, X., & Zhong, S., 1999. Wintertime evolution of the temperature inversion
846 in the Colorado Plateau Basin. *Journal of Applied Meteorology* **38**, 1103–1117.
847 [https://doi.org/10.1175/1520-0450\(1999\)038<1103:WEOTTI>2.0.CO;2](https://doi.org/10.1175/1520-0450(1999)038<1103:WEOTTI>2.0.CO;2)

848 Whiteman, C.D., Hoch, S.W., Horel, J.D., & Charland, A., 2014. Relationship between
849 particulate air pollution and meteorological variables in Utah’s Salt Lake Valley.
850 *Atmospheric Environment* **94**, 742–753. <https://doi.org/10.1016/j.atmosenv.2014.06.012>

851 Whiteman, C.D., Zhong, S., Shaw, W.J., Hubbe, J.M., Bian, X., & Mittelstadt, J., 2001. Cold
852 pools in the Columbia Basin. *Weather and Forecasting* **16**, 432–447.

853 Wilson, T.H. & Fovell, R.G., 2018. Modeling the Evolution and Life Cycle of Radiative Cold
854 Pools and Fog. *Weather and Forecasting* **33**, 203–220. [https://doi.org/10.1175/WAF-D-](https://doi.org/10.1175/WAF-D-17-0109.1)
855 17-0109.1

856 Wolyn, P.G. & McKee, T.B., 1989. Deep Stable Layers in the Intermountain Western United
857 States. *Monthly Weather Review* **117**, 461–472.

858 Yu, L., Zhong, S., & Bian, X., 2017. Multi-day valley cold-air pools in the western United States

859 as derived from NARR. *International Journal of Climatology* **37**, 2466–2476.
860 <https://doi.org/10.1002/joc.4858>

861 Zängl, G., 2005. Wintertime Cold-Air Pools in the Bavarian Danube Valley Basin: Data
862 Analysis and Idealized Numerical Simulations. *Journal of Applied Meteorology and*
863 *Climatology* **44**, 1950–1971.

864 Zanobetti, A., Schwartz, J., Samoli, E., Gryparis, A., Touloumi, G., Peacock, J., Anderson, R.H.,
865 Le Tertre, A., Bobros, J., Celko, M., Goren, A., Forsberg, B., Michelozzi, P., Rabczenko,
866 D., Hoyos, S.P., Wichmann, H.E., & Katsouyanni, K., 2003. The temporal pattern of
867 respiratory and heart disease mortality in response to air pollution. *Environmental Health*
868 *Perspectives* **111**, 1188–1193.

869 Zhong, S., Whiteman, C.D., Bian, X., Shaw, W.J., & Hubbe, J.M., 2001. Meteorological
870 processes affecting the evolution of a wintertime cold air pool in the Columbia Basin.
871 *Monthly Weather Review* **129**, 2600–2613.